Capability of NavIC, an Indian GNSS Constellation, for Retrieval of Surface Soil Moisture

Vivek Chamoli[1, *], Rishi Prakash[1], Anurag Vidyarthi[1], and Ananya Ray[2]

Abstract—Study of Global Navigation Satellite System (GNSS) for various non-navigational applications is gaining importance day by day. Very recently, India's Navigation with Indian Constellation (NavIC) is a new entry in GNSS systems available worldwide such as GPS, GLONASS, Galileo, and Beidou. One of the important non-navigational applications is the study of soil moisture with GNSS. NavIC is very much different from widely used and globally available GPS system. Therefore, in this paper we have analyzed and developed an algorithm for soil moisture retrieval with NavIC Carrier to Noise (C/N_o) ratio. Information of soil moisture is very beneficial for various applications such as groundwater estimation, management of agricultural, drought monitoring and prediction, weather forecasting, and flood forecasting. Amplitude of multipath Carrier to Noise (C/N_o) ratio from the NavIC receiver at L-band has been utilized to determine the soil moisture from smooth bare soil surface. The analyses of sensitivity of soil moisture have been carried out by observing the NavIC multipath data and measurement of in situ soil moisture content. The algorithm development focuses on the retrieval of multipath amplitude from the interference pattern created at the receiver due to direct signal and reflected/multipath signal. The 1st, 2nd, and 3rd order polynomials have been analyzed to detrend the signal before fitting it with sinusoidal variation. It was observed that the multipath amplitude retrieved after detrending the C/N_o data with the 1st order polynomial provides better correlation with observed soil moisture than the 2nd and 3rd order polynomials. An empirical relationship between multipath amplitude and soil moisture has been developed. This developed empirical relationship is capable of providing soil moisture with known multipath amplitude. The retrieved soil moisture with developed algorithm is in good agreement with observed soil moisture with RMSE of 1.43%. Obtained results indicate the promising potential for the estimation of soil moisture with NavIC C/N_o ratio.

1. INTRODUCTION

The measurement of moisture content in the soil is an important area of investigation from the point of view of agricultural, weather monitoring, climate change, soil erosion, soil moisture modeling, and integrated sensing of soil moisture [1–8]. The knowledge of soil moisture (S-M) content in agriculture domain is required because it provides information about the soil health and its suitability for crop production. Furthermore, S-M is used to predict drought in vegetated habitat as well as in soil-vegetation interaction [9, 10], and it plays a vital role in the earthbound water cycle [11, 12]. Conventional S-M observations include specific location measurements. The direct method (utmost authentic) is the gravimetric method. However, this method requires a huge amount of manpower for collecting samples and conducting measurements in the laboratory. Time domain reflectometry (TDR) [13–15] neutron scattering [16–18], gamma-ray scanner, and soil resistivity [19] are also used to measure the S-M. However, the development of remote sensing has provided a robust method for monitoring the spatial

* Corresponding author: Vivek Chamoli (vivekchamoli08@gmail.com).
[1] Department of Electronics & Communication Engineering, Graphic Era Deemed to be University, Dehradun, Uttarakhand, India.
[2] Space Application Center, ISRO, Ahmedabad, India.

distribution, temporal variation, and measurable estimation of soil moisture. Microwave remote sensing is the most impressive technique for S-M estimation. In active microwave remote sensing, the sensor transmits its own signal towards the soil surface, and the reflected signals are measured. However, the naturally emitted microwave radiations from the soil are measured with passive microwave remote sensing. The study of soil moisture with active microwave remote sensing is very complex whereas passive microwave remote sensing provides the soil moisture estimation at large spatial resolution which ranges from 10 to 100 km.

The spatial resolution in Global Navigation Satellite System (GNSS) is generally quantified as an ellipse due to the projection of the first Fresnel zone or Fresnel reflection coefficient of active region [19]. The range of spatial resolution (i.e., 10–100 m) in GNSS used to retrieve soil moisture is highly reliant on a range of variables, many related to the height of the receiver [20], topographic variations [21], and the existence of the surface observed [19–22]. The study of earth surfaces characteristic with the Navigation Satellite System was first proposed approximately 20 years ago. Initially, it was proposed that the receiver must be specially designed to capture the reflected signal to predict the soil moisture condition. However, recent studies have demonstrated that the existing ground-based navigation receiver can be used to sense the soil moisture. It was observed that the signal strength correlates with precipitation and dry down situation of installed receiver site. Studies to monitor the soil moisture with navigation satellites have been mostly carried out with Global Positioning System (GPS). The basic principle involved in the sensing of soil moisture with Global Navigation Satellite System (GNSS) is the variability of soil dielectric constant with water content available in the soil. Higher water content in soil raises the dielectric constant of soil to a higher value which results in increased reflectivity of GNSS signal from the ground [23–25].

Larson et al. [23, 26] have investigated multipath signals from Global Positioning System to analyze land surface aspects such as snow deepness, S-M and vegetation moisture content around GNSS antennas. Researchers have taken advantage of multipath reflections from the soil surface to determine the S-M content. Larson et al. [26] observed that the GPS signal-to-noise ratio was horizontally and 1–6 cm vertically sensitive to soil moisture variations over an area of 1000 m^2. The authors have shown that GPS signals penetrate more deeply into dry soil than wet soil. This penetration changes as well as changing the dielectric constant; the GPS signal strength changes its frequency and amplitude of the signal. Roussel et al. [27] proposed a GNSS-reflectometry interference pattern technique for GPS and GLONASS based on the amplitude of multipath signal, phase of multipath signal, and effective height of the antenna to determine temporal variation in Yang et al. [28] studied the feasibility of SNR data from China's BeiDou Navigation Satellite System (BDS) for the estimation of soil moisture. The authors did not provide any retrieval algorithm; however, they showed the variation in multipath amplitude and phase with change in soil moisture. A comparison of BDS multipath signal sensitivity towards S-M and GPS multipath signal sensitivity towards S-M has also been carried out. It has been shown that GPS data is, in general, more sensitive to small precipitation than BDS data. Han et al. [29] studied the GNSS-IR technique to develop the semi-empirical model. The main idea of this model is to approximate the direct and reflected signal by a second order and fourth order polynomial, respectively, based on the well established SNR model.

Various other researchers have also examined the feasibility of retrieving S-M with GNSS data [23, 26–41]. They have found that low elevation angles are more useful than high elevation angles (greater than 30°), in the study of S-M's effect on multipath data.

Indian Regional Navigational Satellite System (IRNSS) popularly known as Navigation with Indian Constellation (NavIC) is owned by Indian government. The architecture of the traditional GNSS system is based on three segments which are space, user, and ground. The same concept has been used in IRNSS. Total 7 satellites have been used for the navigation in IRNSS space segment. 3 out of 7 satellites are located in geo-stationary orbit (GEOs) at 83° East, 32.5° East, and 131.5° East longitude. 4 satellites are in geo-synchronous orbit (GSOs) in which two satellites are located at 111.75° East, and the other two are located at 55° East (https://directory.eoportal.org/web/eoportal/satellite-missions/i/irnss). The IRNSS ground segment consists of IRNSS Space Craft Control Centre (SCC), IRNSS Range and Integrity Monitoring Stations (IRIMS), Laser Ranging Station (ILRS), IRNSS Navigation Centre (INC), IRNSS CDMA Ranging Stations (IRCDR), IRNSS TTC and Uplinking Stations (IRTTC), Data Communication Network

(IRDCN) and IRNSS Timing Centre (IRNWT) (https://www.isro.gov.in/irnss-programme). The single/dual-frequency (L5 and S1 bands) receiver has been used in IRNSS space segment. IRNSS provides two kinds of services. The first is Special Positioning Service, and the second is Precision Services.

A comparison of GPS and IRNSS reveals that GPS has 31 satellites while IRNSS is on the go with 7 satellites. IRNSS has 2 constellations, geo-synchronous satellites, and geo-stationary satellite; however, GPS has only one constellation, i.e., Medium Earth or-bit (MEO). IRNSS will provide standard positioning service to all users with a posi-tion accuracy of 5 m. The GPS, on the other hand, has a position accuracy of 20–30 m (https://directory.eoportal.org/web/eoportal/satellite-missions/i/irnss). Frequency bands for IRNSS are L5 (1176.45 MHz) and S1 (2492.028 MHz) (https://www.isro.gov.in/irnss-programme; https://www.isro.gov.in/irnss-programme) whereas for GPS, it is L1 (1575.42 MHz) and L2 (1227.60 MHz) (https://www.gps.gov/).

This paper is divided into four sections. Section 1 provides the introduction of the work carried out and NavIC constellation. The selection of NavIC satellite with the concept of soil moisture measurement, experimental setup, brief discussion about ground truth data collection, and modeling approach is shown in Section 2. The experimental result derived from NavIC $C/N_\circ$ data and steps for developing the algorithms and validation of algorithm are discussed in Section 3. Finally, conclusion is drawn in Section 4.

2. MATERIAL AND METHODS

2.1. Selection of NavIC Satellite to Determine the Sensitivity of Soil Moisture for $C/N_\circ$ Ratio

NavIC constellation consists of three Geostationary and four Geosynchronous satellites. In this paper, the change in $C/N_\circ$ with change in elevation angle is observed to determine the surface soil moisture. The change in $C/N_\circ$ with the change in elevation angle can be obtained with geosynchronous satellites (NavIC-1, NavIC-2, NavIC-4, and NavIC-5). The locations of geostationary satellites (NavIC-3, NavIC-6, and NavIC-7) are fixed with respect to receiver location. The elevation angle of NavIC-1 and NavIC-2 changes from 18.94° to 68°, whereas the change in elevation angle for NavIC-4 and NavIC-5 is 13.70° to 58°. Several researchers have shown that lower elevation angles are useful for analyzing the sensitivity of soil moisture by observing $C/N_\circ$ ratio of GNSS receiver [23, 26–41].

Therefore, in this paper, we have analyzed NavIC-4 data up to 30° elevation angle to observe the sensitivity of soil moisture with $C/N_\circ$. Fig. 1 shows the sky plot of geosynchronous satellites. NavIC-1 and NavIC-2 follow the same path whereas NavIC-3 and NavIC-4 also follow the same path, but this path is different from NavIC-1 and NavIC-2.

2.2. Selection of Receiver Height and Area for Ground Truth Soil Sample Collection

Selection of receiver height is another important aspect of the work. The height of the receiver directly affects the multipath fluctuation of NavIC data. It was observed that most of the researchers have preferred to keep the receiver at a height of 2 m, 2.5 m, or 3 m [23–41]. Therefore, in this work, we set the receiver height at 2 m. Fig. 2 shows the radial distance of reflection point from the receiver base with the change in elevation angle for different receiver heights. It can be observed from Fig. 2 that increasing the height of the receiver will also increase the coverage area of the reflected signal. Further, it can be observed from Fig. 2 that the reflection point on the ground from the receiver decreases with the increases in elevation angle, i.e., reflection point is very close to the receiver for high elevation angles whereas it is much far away from the receiver for low elevation angles.

2.3. Concept of Soil Moisture Measurement with NavIC Signal

The basic geometry of NavIC multipath is shown in Fig. 3. Signal received from the antenna can be split into a direct and reflected component. As the satellite signal is tracked, the direct and reflected signals
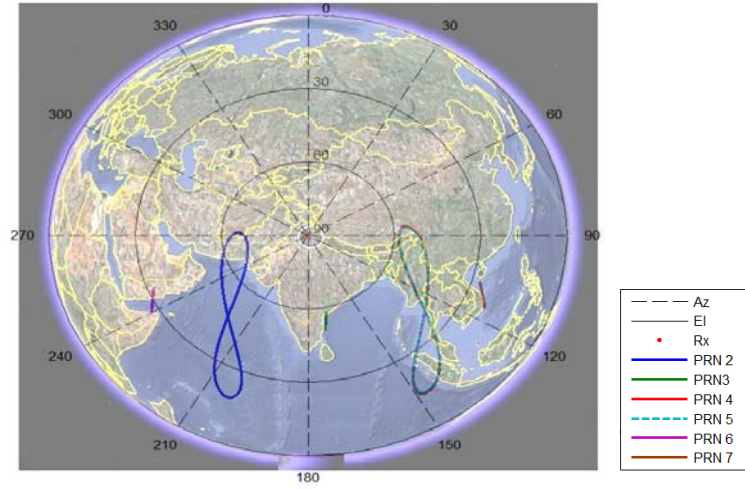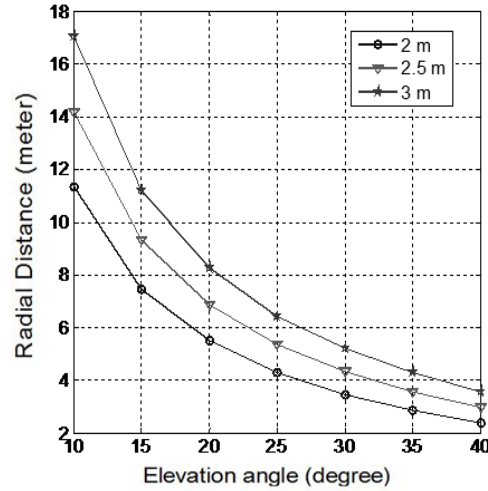
Figure 1. Sky plot of NavIC satellites.

Figure 2. Ground Reflection distance of from the receiver at different elevation angle and at different antenna height.

go in and out of phase, causing constructive and destructive interferences. For a planar horizontal reflector, the signature of this interference is a sine wave of constant frequency that depends on the height of the antenna above the reflector, the NavIC frequency, and sine of the elevation angle (θ). C/N$_\circ$ changes generate amplitude variations which are based on the reflection and the dielectric content of the soil.

Assuming the horizontal terrain surface, the extra distance (δ) traveled by the signal as shown in Fig. 3 is given as

$$\delta = 2\hbar\sin\theta \tag{1}$$

where θ is the elevation angle, and the height of the receiver is $\hbar$ from the ground. The path difference between direct and multipath signals results in a phase difference which can be expressed as

$$\psi = \frac{2\pi}{\lambda} \times \delta = \frac{4\pi h}{\lambda}\sin\theta \tag{2}$$

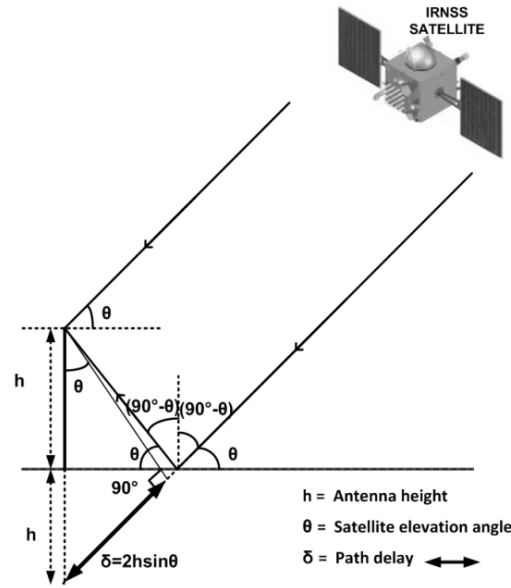where λ is the incoming satellite signal wavelength.

Figure 3. The multipath geometry of NavIC signal.

The multipath frequency can be written as:

$$\omega = \frac{d\psi}{dt} = \frac{4\pi h}{\lambda} \cos \frac{d\theta}{dt} \tag{3}$$

The antenna height therefore directly affects the frequency of the multipath. Antenna far above the ground surface will have higher multipath frequency than antennas closer to reflecting surface. If we consider $\sin\theta$ as a variable, then the multipath frequency can be written as

$$\frac{d\psi}{d(\sin\theta)} = \frac{4\pi \hbar}{\lambda} \tag{4}$$

The modified frequency is constant for a horizontal surface. Using an independent variable sine of elevation angle, the multipath frequency becomes proportional to $\hbar$ (height of receiver) only as all other parameters are constant for NavIC system. The multipath C/N_o can be expressed as

$$C/N_{mpi} = V_{mpi} \cos \left[\frac{4\pi h}{\lambda} \sin\theta + \varphi_{mpi} \right] \tag{5}$$

where V_{mpi} is the multipath amplitude, and φ_{mpi} is the multipath phase. Many authors have used Eq. (5) to determine the value of multipath amplitude and multipath phase for the study of soil moisture with GNSS [23, 26–41].

2.4. NavIC Receiver Installation and Ground Truth Data Collection

2.4.1. Receiver Installation

In the Graphic Era (Deemed to be University), Dehradun, Uttarakhand, India, the NavIC receiver is installed. The data collection with NavIC receiver has been made in the playground, whose central latitude and longitude are $30°16'05''$ N and $77°59'35''$ E, respectively as shown in Fig. 4. The surface of the ground is smooth, and the size of the ground is approximately $6,899\,\mathrm{m}^2$.

2.4.2. Ground Truth Data Collection for Soil Moisture Measurement

Ground measurement of soil moisture is necessary to develop the relationship between soil moisture and NavIC C/N_o ratio. We have collected 15 soil samples from $500\,\mathrm{m}^2$ area around the antenna. The depth

Figure 4. Google earth image of the study area (GEU ground).

of the collected soil samples was 5 to 10 cm. $500 \, \text{m}^2$ area around the antenna for soil sample collection is in accordance with Section 2.1.

To determine the gravimetric soil moisture, the weight of moist soil samples collected from the ground was measured firstly. Then, these soil samples were kept in an oven at $105°\text{C}$ for 24 hours, and the weights of dry (moisture free) soil samples were measured. The average value of soil moisture from these 15 soil samples was estimated which was considered as gravimetric soil moisture of a single day. Similar procedure was carried out for each day of observation.

The gravimetric soil moisture was evaluated as:

$$G_v = \frac{S_{moist} - S_{dry}}{S_{dry}} \times 100 \tag{6}$$

where S_{dry} and S_{moist} are the weight of dry soil and the weight of moist (wet) soil, respectively. The minimum and maximum soil moistures observed during the experiment were 9.25% and 31.85%, respectively. Averages of 15 soil samples were taken into account for determination of soil moisture. The standard deviation for soil moisture was approximately 1.82.

2.5. Modeling Approach

Major work to retrieve soil moisture with the GNSS has been carried out with GPS. Most of the paper which retrieves soil moisture using single antenna follows the concept of GNSS interferometry, i.e., the analysis of interference pattern constructed from direct and reflected/multipath signals. As a first step of analysis, researchers suggest the low order polynomial to detrend the data. However, very few researchers have specified the exact order of polynomial to be used in the analysis. Further, the order of polynomial may vary from GPS to NavIC, while the soil moisture is studied. This may be due to the time taken during observation. GPS elevation changes from $15°$ to $30°$ in approximately 2 hours whereas NavIC takes approximately 5 hours for the same range of elevation angle. Therefore, it is very much necessary to study the order of polynomial as well as to develop the algorithm for retrieval of soil moisture with NavIC signal. In comparison to GPS where we utilize $5°$ to $30°$ elevation angle in soil moisture retrieval studies, in NavIC we can only utilize $15°$ to $30°$ elevation angle as the NavIC satellites are geosynchronous satellites. The data analyzed in the work are of NavIC-4 where minimum elevation angle is $13.7°$, and maximum is $58°$. The following steps explain the detailed methodology to find the order of polynomial suitable for NavIC satellite and algorithm to determine soil moisture with NavIC data.

Step 1: As per Eq. (5) the interference pattern plotted against sine of elevation angle provides constant frequency. Therefore, the data originally with respect to elevation angle were converted in sine of elevation angle. Low pass filter was also applied to remove the fast variation in the signal.

Step 2: The direct power received by the NavIC receiver increases with the increase in elevation angle. The increases in direct power due to the increase in elevation angle occur because of decreased distance between the NavIC satellite and NavIC receiver. Therefore, an increasing trend in C/N_o multipath oscillations with elevation angle is observed. To mitigate these increasing trends, detrending of C/N_o data has to be carried out. First, the second and third order polynomials are analysed to detrend the C/N_o multipath data.

Step 3: The detrended data are fitted with sine curve with the Least Square Estimation method to provide the multipath amplitude. Three different values of multipath amplitude are obtained for single date data due to three different order polynomials used in the detrending.

Step 4: Regression analysis is carried out to develop an empirical relationship between the amplitude retrieved in previous step and ground truth soil moisture obtained from in-situ measurement. The coefficient of determination (R^2) and Root Mean Square Error (RMSE) were evaluated to determine the best model to retrieve soil moisture. It was observed that the detrended data with the 1st order polynomial and empirical relationship with second order polynomial provide maximum R^2 and minimum RMSE.

Step 5: The validation of developed empirical relationship was carried out with the different sets of data that were not used in the development phase. RMSE was evaluated to determine the difference between the soil moisture obtained with developed model and ground truth observations.

3. RESULT AND DISCUSSION:

3.1. Retrieval of Multipath Amplitude

NavIC receiver provides C/N_o, PR (pseudo range), Elevation angle, satellite X, Y, Z coordinate position, Doppler frequency, azimuth angle, and some other parameters. In this paper, C/N_o data are utilized to determine the surface soil moisture. Multipath amplitude and phase are determined by analyzing the C/N_o data received from the NavIC geosynchronous satellite. The range in multipath can be attributed to the effect of dielectric constant which changes due to the change in amount of moisture content in
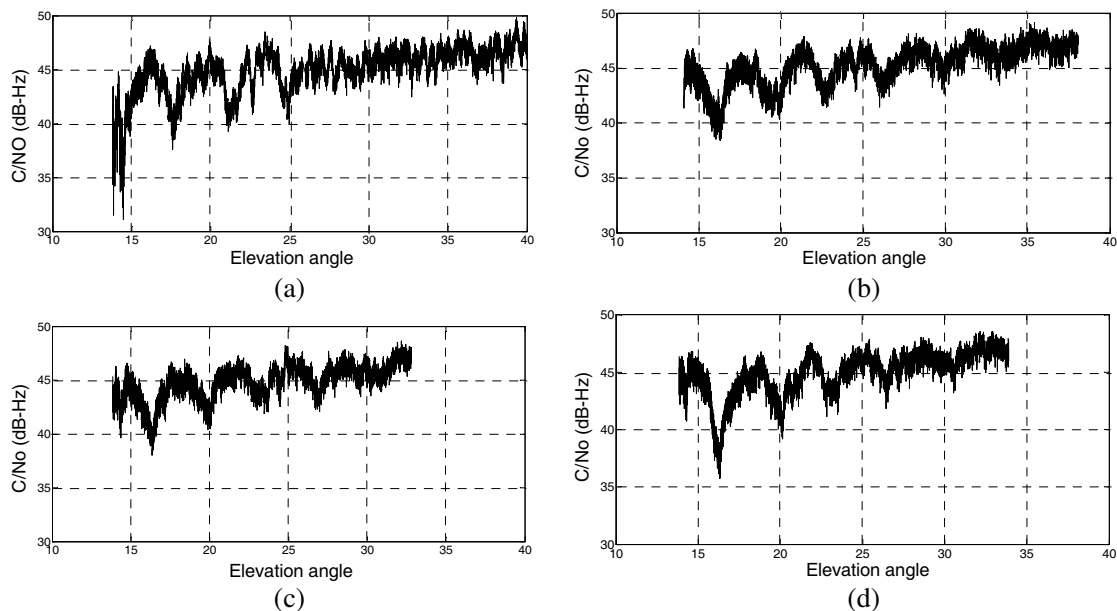

Figure 5. Raw C/N_o data form NavIC receiver on date, (a) 04/09/2017, (b) 06/06/2018, (c) 14/06/2018 and (d) 24/06/2018.
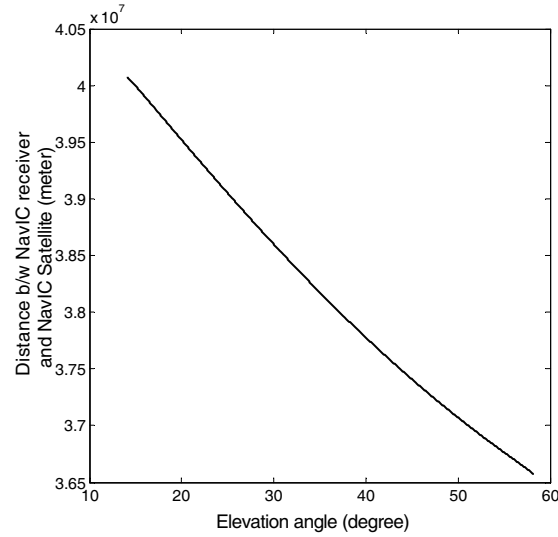
Figure 6. Change in distance between NavIC receiver and NavIC satellite with change in elevation angle.
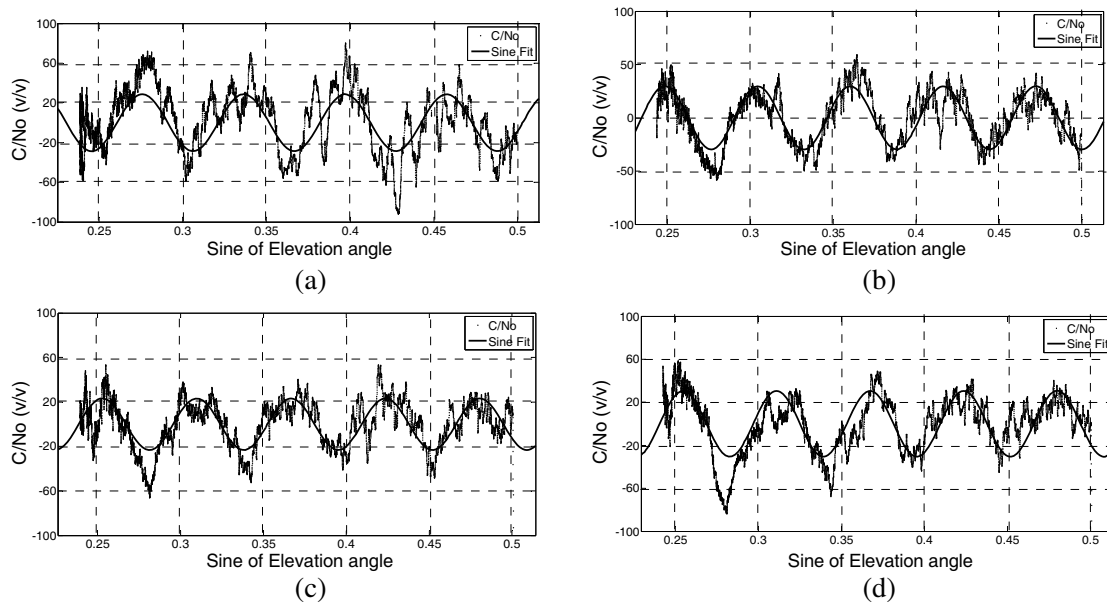

Figure 7. Sinusoidal least square estimated curve for Linear fitting on dates, (a) 04/09/2017, (b) 06/06/2018, (c) 14/06/2018 and (d) 24/06/2018.

soil. The raw C/N_o data received from NavIC-4 satellite are plotted with the elevation angle as shown in Figs. 5(a), (b), (c), and (d). It can be observed from the figures that the interference pattern in C/N_o becomes less significant at higher elevation angles (i.e., greater than $30°$) than lower elevation angle (i.e., less than $30°$). Similar observations have also been observed with GPS, GLONASS, and BeiDou [23, 26–39]. Therefore, lower elevation angles ($\leq 30°$) are utilized in this study for the retrieval of soil moisture with NavIC multipath signal. Fast oscillations can also be observed in the extracted C/N_o data along with the multipath oscillations as shown in Fig. 5. The fast oscillation represents the noise in receiver and is superimposed on the multipath interference. A low pass filter is used to remove these fast variations. The frequency of multipath oscillation as observed in Fig. 5 is the function of elevation angle as explained by Eq. (3). Multipath frequency being the function of elevation angle changes with the

change in elevation. Therefore, we plot NavIC C/N_o with sine of elevation angle to make the frequency of multipath oscillations independent of the elevation angle as suggested by Eq. (4). C/N_o in dB-Hz is also converted to volts/volts in accordance with Eq. (5). The direct power received by the NavIC receiver increases with the increase in elevation angle. The increase in direct power due to the increase in elevation angle occurs because of decreased distance between the NavIC satellite and NavIC receiver as shown in Fig. 6. A change of 1660 km is observed when the elevation angle changes from 13.7° to 30°. Therefore, an increasing trend in C/N_o multipath oscillations can be observed in Fig. 5. To mitigate
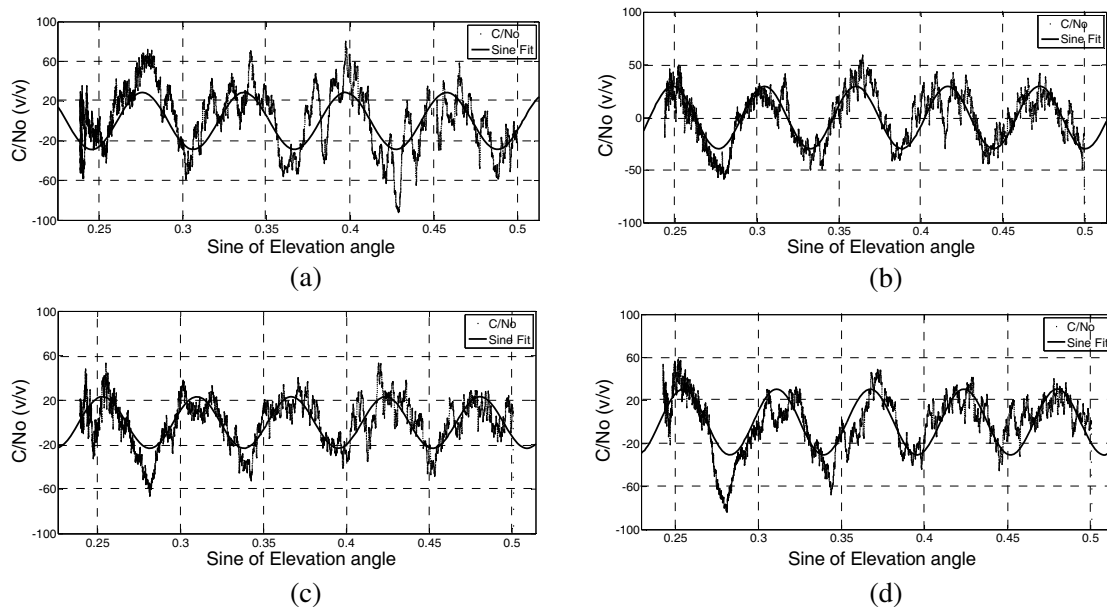

Figure 8. Sinusoidal least square estimated curve for Quadratic fitting on dates, (a) 04/09/2017, (b) 06/06/2018, (c) 14/06/2018 and (d) 24/06/2018.
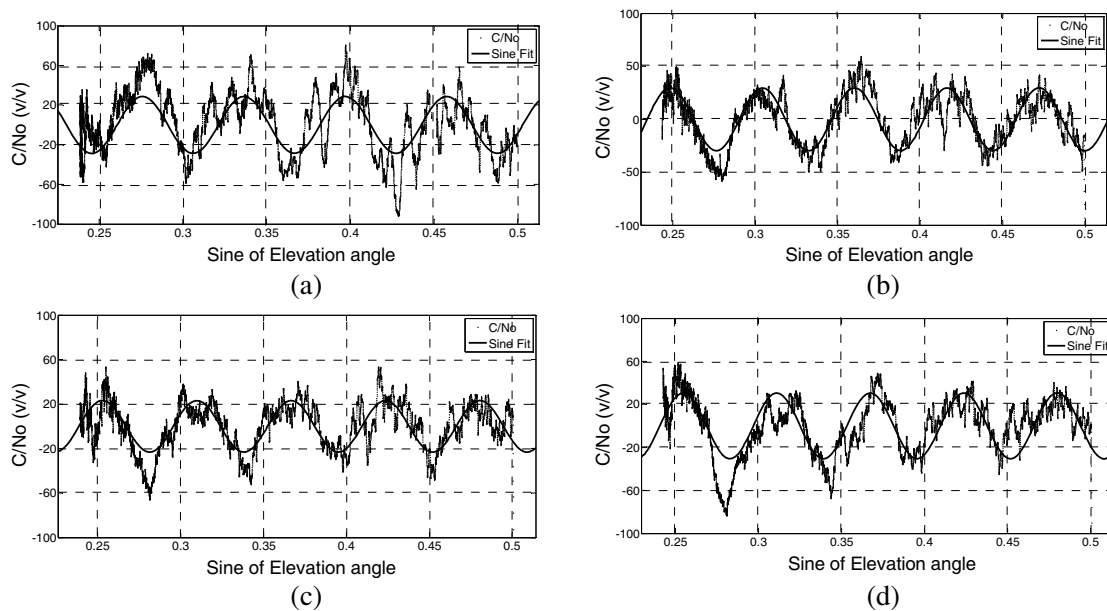

Figure 9. Sinusoidal least square estimated curve for Cubic fitting on dates, (a) 04/09/2017, (b) 06/06/2018, (c) 14/06/2018 and (d) 24/06/2018.

these increasing trends, detrending of C/N_o data is carried out by applying three different approaches: the first one is Linear fit (1st order polynomial); the second is Quadratic fit (2nd order polynomial); and the third is the Cubic fit (3rd order polynomial). The aim of studying different order polynomials fit is to determine the best empirical approach for the retrieval of soil moisture with C/N_o data received from NavIC receiver. The determination of residual from the received C/N_o from the NavIC receiver is important for the estimation of multipath amplitude. This multipath amplitude depends on the approach which it has been evaluated, i.e., by fitting polynomial of the 1st order, polynomial of the 2nd order or polynomial of the 3rd order.

Least square estimation method has been used to determine the multipath amplitude and multipath phase as provided by Eq. (5). Multipath amplitude is used in this study. Fig. 7, Fig. 8, and Fig. 9 show sinusoidal least square estimated curves on the Linear fitted data, Quadratic fitted data and Cubic fitted data, respectively. The curve fitting provides the amplitude of sine fit, which was used to develop the relationship with ground truth soil moisture. The amplitude of the NavIC data for Linear fitting has been determined 27.82 (V/V), 30.62 (V/V), 23.18 (V/V), and 26.7 (V/V), for soil moisture 24%, 20.95%, 15.12%, and 17.27%, respectively, as shown in Fig. 7. The amplitude of the NavIC data for Quadratic fitting has been determined 25.5 (V/V), 29.63 (V/V), 22.62 (V/V), and 25.95 (V/V), for soil moisture 24%, 20.95%, 15.12%, and 17.27%, respectively, as shown in Fig. 8. The amplitude of the
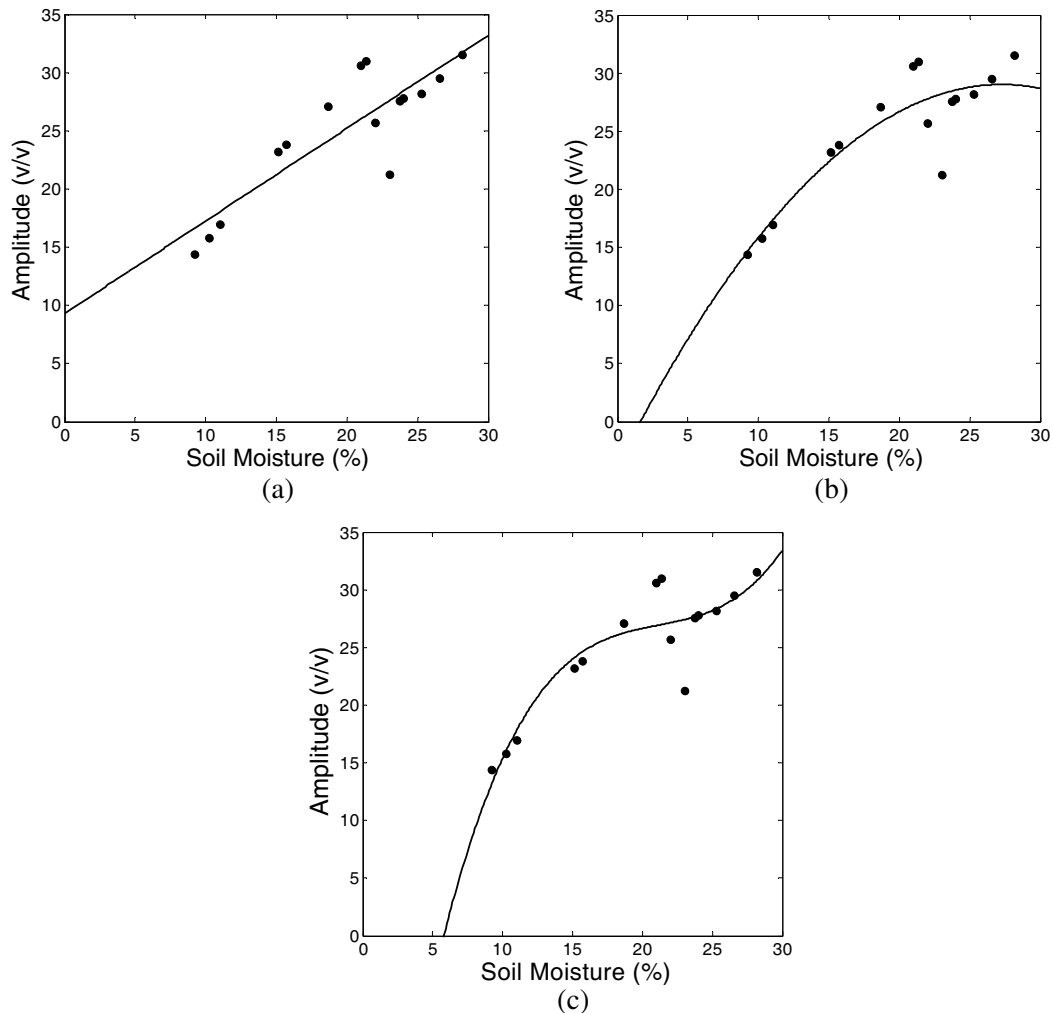

Figure 10. Shows the multipath amplitude variation for soil moisture changes for (a) Linear Model with 1st order polynomial fit, (b) Linear Model with 2nd order polynomial fit and (c) Linear Model with 3rd order polynomial fit.

NavIC data for Cubic fitting has been determined 24.47 (V/V), 27.73 (V/V), 22.25 (V/V), and 23.26 (V/V), for soil moisture 24%, 20.95%, 15.12%, and 17.27%, respectively, as shown in Fig. 9.

3.2. Development of Empirical Relationship between Multipath Amplitude and Soil Moisture

We had analyzed the data from NavI-4 for 26 days. During our observations, S-M varied from 9.25% to 31.85% and corresponding amplitude varied from 13.97 V/V to 37.51 V/V for Linear Model, 13.60 V/V to 37.99 V/V for Quadratic Model, and 16 V/V to 35.55 V/V for Cubic Model. The aim of this study is to determine the soil moisture with multipath amplitude. Therefore, in the next step, we discuss the development of empirical relationships between S-M and multipath amplitude. Fig. 10 shows the variation of multipath amplitude and soil moisture. The multipath amplitude has been retrieved with linear model as discussed in previous section. Figs. 10(a), (b), and (c) show the fitted curve with polynomial of the 1st order, polynomial of the 2nd order, and polynomial of the 3rd order, respectively. The fittings of different order polynomials have been carried out to determine the relationship between soil moisture and multipath amplitude. Similarly, Figs. 11 and 12 show the variation and fitting of curves
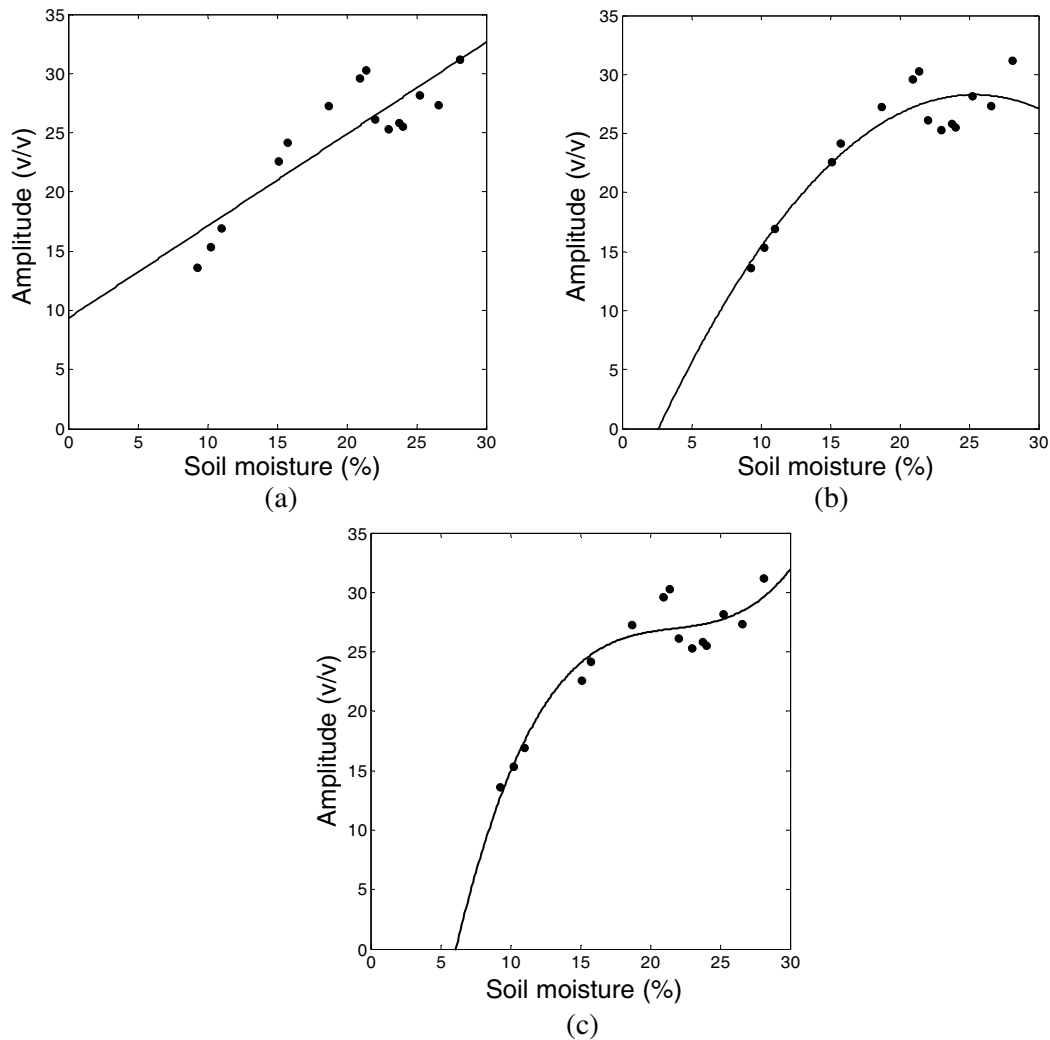

(a)

(b)

(c)

Figure 11. Shows the multipath amplitude variation for soil moisture changes for (a) Quadratic Model with 1st order polynomial fit, (b) Quadratic Model with 2nd order polynomial fit and (c) Quadratic Model with 3rd order polynomial fit.

when the multipath amplitude is retrieved through Quadratic model and Cubic mode, respectively.

Table 1 shows the coefficient of determination (R^2) and Root Mean Square Error (RMSE) of different models discussed and shown in Figs. 10, 11, and 12. It can be clearly observed form Table 1 that Linear model with the 2nd order polynomial fit provides the highest value of R^2, i.e., 0.89 and minimum value of RMSE, i.e., 1.82 as compared to other models. Therefore, an empirical equation can be developed between multipath amplitude retrieved through linear model and observed soil moisture as shown in Fig. 10(b). Eq. (7) provides the empirical relation between soil moisture and multipath amplitude retrieved through Linear Model with the 2nd order polynomial fit

$$A_m = a * SMC^2 + b * SMC - c \tag{7}$$

where a, b, and c are the empirical constants; SMC is the soil moisture in percentage; and A_m is the amplitude in volt/volt of the multipath signal. Values of empirical constants a, b, and c are -0.05, 2.7, and 6.2, respectively.
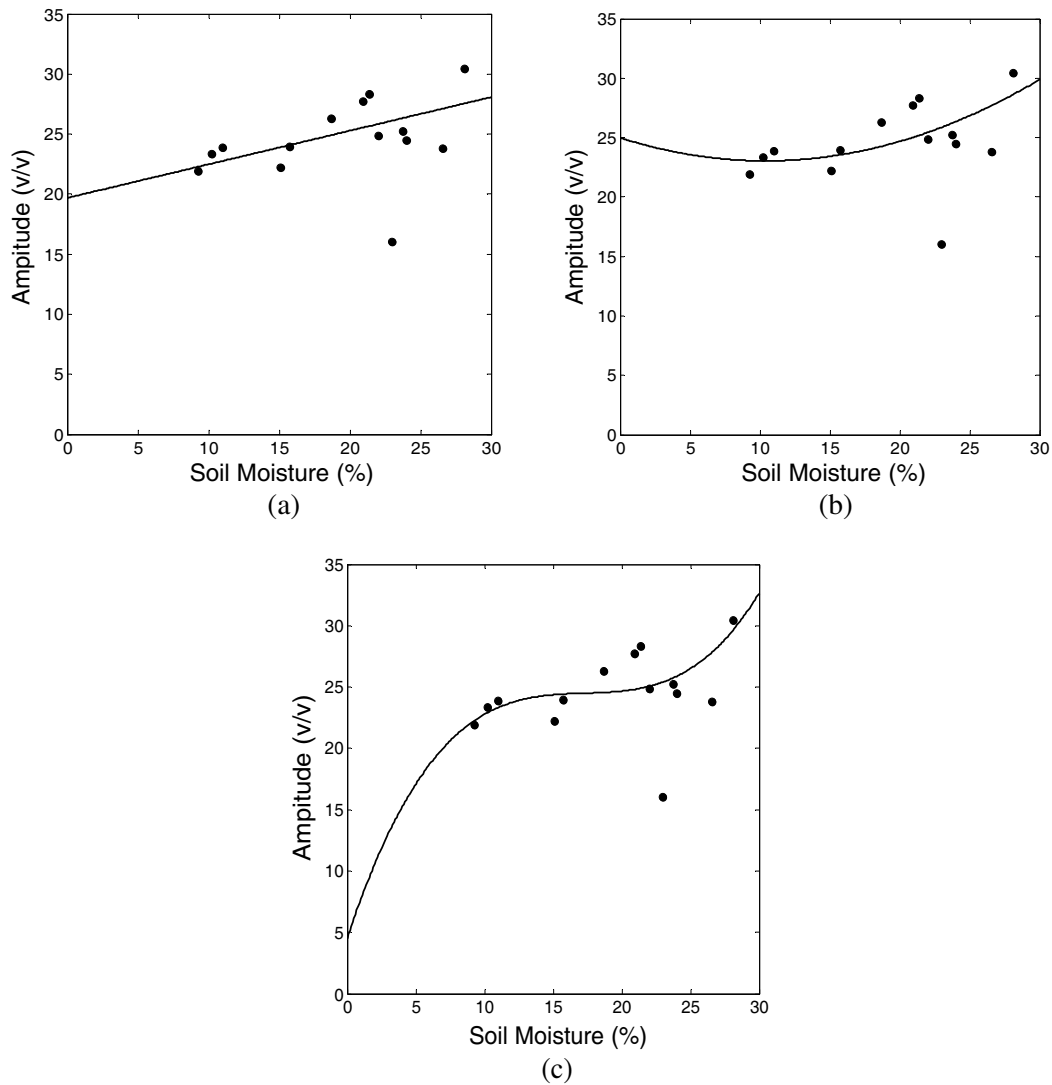

Figure 12. Shows multipath amplitude variation for soil moisture changes for (a) Cubic Model with 1st order polynomial fit, (b) Cubic Model with 2nd order polynomial fit and (c) Cubic Model with 3rd order polynomial fit.

Table 1. The coefficient of determination (R^2) and Root Mean Square Error (RMSE) for different models.

Model Name	R^2	RMSE (%)
Linear Model with 1st order polynomial fit	0.82	2.37
Linear Model with 2nd order polynomial fit	0.89	1.82
Linear Model with 3rd order polynomial fit	0.83	2.60
Quadratic Model with 1st order polynomial fit	0.77	2.64
Quadratic Model with 2nd order polynomial fit	0.87	2.06
Quadratic Model with 3rd order polynomial fit	0.88	1.84
Cubic Model with 1st order polynomial fit	0.15	4.09
Cubic Model with 2nd order polynomial fit	0.17	4.21
Cubic Model with 3rd order polynomial fit	0.19	4.35

3.3. Validation of an Empirically Developed Model

The data were collected for 26 days in the month of September 2017, June 2018, and July 2018. 15 days data set was used to develop an empirical relationship between amplitude of the multipath signal and soil moisture as explained in Section 3.2. The remaining 11 days data were utilized to validate the algorithm. Algorithms developed in Section 3.2 have been utilized to obtain the amplitude of multipath data, and Eq. (7) was employed to obtain the corresponding soil moisture. The retrieval of soil moisture from Eq. (7) with given multipath amplitude has been carried out by utilizing the *fsolve* function available in MATLAB. Fig. 13 shows the relationship between the retrieved soil moisture from developed algorithm and observed gravimetric soil moisture. The RMSE from developed relationship is 1.43 %.
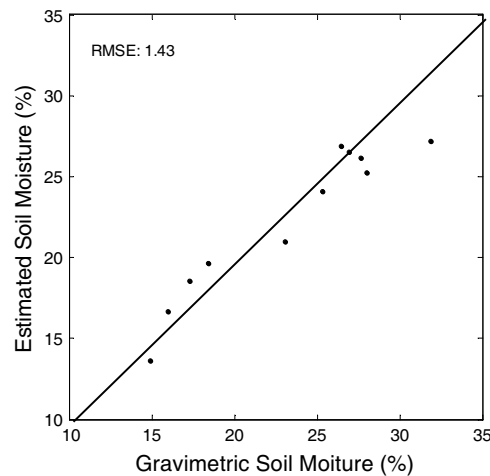
Figure 13. Shows the relationship between the estimated S-M from NavIC data and gravimetric S-M for Linear Model with 2nd order polynomial fit.

4. CONCLUSION

Recently, developed India's navigational satellite system, i.e., NavIC, is different in several aspects in comparison to widely used GPS system as well as other GNSS systems as explained in previous sections. Therefore, this study has focused on the sensitivity analysis of NavIC multipath signal for the change in surface soil moisture and its retrieval. The analyses of observed data showed that the multipath

amplitude increased with the increase in soil moisture. The relationship of soil moisture with multipath amplitude has shown high dependency on the measurement methodology of multipath amplitude of the received C/N_o from NavIC receiver. The study of multipath amplitude was carried out for NavIC-4 geo-synchronous satellite because its elevation angle changed from $13.7°$ to $58°$ which covered the desired range of elevation angle, i.e., $15°$ to $30°$ used in this study. Determination of multipath amplitude from received C/N_o requires the detrending of data which was carried out with the 1st order, 2nd order, and 3rd order polynomials. The developed retrieval algorithm shows that multipath amplitude retrieved trough the 1st order polynomial provides better result than the amplitude retrieved through the 2nd order polynomial and 3rd order polynomial. The empirical relationship between multipath amplitude retrieved through different order polynomials and soil moisture was analyzed based on the coefficient of determination and RMSE. A quadratic relationship was observed between soil moisture and multipath amplitude which was retrieved through the 1st order polynomial. *fsolve* function available in Matlab was utilized to retrieve the soil moisture from multipath amplitude. The retrieved soil moisture with developed algorithm and ground truth soil moisture was found in good agreement with RMSE of 1.43%. This is the first of its kind of study for sensitivity analysis and soil moisture retrieval with NavIC signal. This study can be very useful for long term and daily study of soil moisture at any specific study area for environmental modeling, agriculture, hydrological modeling, etc.

ACKNOWLEDGMENT

REFERENCES

1. Prakash, R., D. Singh, and N. P. Pathak, "Microwave specular scattering response of soil texture at X-band," *Adv. Space Res.*, Vol. 44, No. 7, 801–814, 2009.
2. Wan, W., H. Li, X. Chen, P. Luo, and J. Wan, "Preliminary calibration of GPS signals and its effects on soil moisture estimation," *Acta Meteor. Sinica*, Vol. 27, No. 2, 221–232, 2013.
3. Phillips, A. J., N. K. Newlands, S. H. Liang, and B. H. Ellert, "Integrated sensing of soil moisture at the field-scale: Measuring, modeling and sharing for improved agricultural decision support," *Comput. Electron. Agr.*, Vol. 107, 73–88, 2014.
4. Liang, W. L., F. X. Hung, M. C. Chan, and T. H. Lu, "Spatial structure of surface soil water content in a natural forested headwater catchment with a subtropical monsoon climate," *J. Hydrol.*, Vol. 516, 210–221, 2014.
5. Tabibi, S., F. G. Nievinski, T. van Dam, and J. F. Monico, "Assessment of modernized GPS L5 SNR for ground-based multipath reflectometry applications," *Adv. Space Res.*, Vol. 55, No. 4, 1104–1116, 2015.
6. Zhang, D., Z. L. Li, R. Tang, B. H. Tang, H. Wu, J. Lu, and K. Shao, "Validation of a practical normalized soil moisture model with in situ measurements in humid and semi-arid regions," *Int. J. Remote Sens.*, Vol. 36, Nos. 19–20, 5015–5030, 2015.
7. El Hajj, M., N. Baghdadi, M. Zribi, G. Belaud, B. Cheviron, D. Courault, and F. Charron, "Soil moisture retrieval over irrigated grassland using X-band SAR data," *Remote Sensing of Environment*, Vol. 176, 202–218, 2016.
8. Liao, W., D. Wang, G. Wang, Y. Xia, and X. Liu, "Quality control and evaluation of the observed daily data in the north american soil moisture database," *J. Meteor. Res.*, Vol. 33, No. 3, 501–518, 2019.
9. Pitman, A. J., "The evolution of, and revolution in, land surface schemes designed for climate models," *Int. J. Climatol.*, Vol. 23, No. 5, 479–510, 2003.
10. Istanbulluoglu, E. and R. L. Bras, "On the dynamics of soil moisture, vegetation, and erosion: Implications of climate variability and change," *Water Resour. Res.*, Vol. 42, No. 6, 1–17, 2006.

11. Rodriguez-Alvarez, N., A. Camps, M. Vall-Llossera, X. Bosch-Lluis, A. Monerris, I. Ramos-Perez, E. Valencia, J. F. Marchan-Hernandez, J. Martinez-Fernandez, G. Baroncini-Turricchia, and C. Perez-Gutierrez, "Land geophysical parameters retrieval using the interference pattern GNSS-R technique," *IEEE Transactions on Geoscience and Remote Sensing*, Vol. 49, No. 1, 71–84, 2011.

12. Bogena, H. R., J. A. Huisman, C. Oberdörster, and H. Vereecken, "Evaluation of a low-cost soil water content sensor for wireless network applications," *J. Hydrol.*, Vol. 344, Nos. 1–2, 32–42, 2007.

13. Ledieu, J., P. De Ridder, P. De Clerck, and S. Dautrebande, "A method of measuring soil moisture by time-domain reflectometry," *J. Hydrol.*, Vol. 88, Nos. 3–4, 319–328, 1986.

14. Robinson, D. A., S. B. Jones, J. M. Wraith, D. Or, and S. P. Friedman, "A review of advances in dielectric and electrical conductivity measurement in soils using time domain reflectometry," *Vadose Zone J.*, Vol. 2, No. 4, 444–475, 2003.

15. Cristi, F., V. Fierro, F. Suárez, J. F. Muñoz, and M. B. Hausner, "A TDR-waveform approach to estimate soil water content in electrically conductive soils," *Comput. Electron. Agr.*, No. 121, 160–168, 2016.

16. Elder, A. N. and T. C. Rasmussen, "Neutron probe calibration in unsaturated tuff," *Soil Sci. Soc. Am. J.*, Vol. 58, No. 5, 1301–1307, 1994.

17. Li, J., D. W. Smith, and S. G. Fityus, "The effect of a gap between the access tube and the soil during neutron probe measurements," *Soil Res.*, Vol. 41, No. 1, 151–164, 2003.

18. Sreedeep, S., A. C. Reshma, and D. N. Singh, "Measuring soil electrical resistivity using a resistivity box and a resistivity probe," *Geotech. Test. J.*, Vol. 27, No. 4, 411–415, 2004.

19. Masters, D., P. Axelrad, and S. Katzberg, "Initial results of land-reflected GPS bistatic radar measurements in SMEX02," *Remote Sensing of Environment*, Vol. 92, No. 4, 507–520, 2004.

20. Camps, A., "Spatial resolution in GNSS-R under coherent scattering," *IEEE Geoscience and Remote Sensing Letters*, Vol. 17, No. 1, 32–36, 2019.

21. Gleason, S., A. O'Brien, A. Russel, M. M. Al-Khaldi, and J. T. Johnson, "Geolocation, calibration and surface resolution of CYGNSS GNSS-R land observations," *Remote Sensing*, Vol. 12, No. 8, 1317, 2020.

22. Balakhder, A. M., M. M. Al-Khaldi, and J. T. Johnson, "On the coherency of ocean and land surface specular scattering for GNSS-R and signals of opportunity systems," *IEEE Transactions on Geoscience and Remote Sensing*, Vol. 57, No. 12, 10426–10436, 2019.

23. Larson, K. M., E. E. Small, E. D. Gutmann, A. L. Bilich, J. J. Braun, and V. U. Zavorotny, "Use of GPS receivers as a soil moisture network for water cycle studies," *Geophys. Res. Lett.*, Vol. 35, No. 24, 1–5, 2008.

24. Katzberg, S. and J. Garrison, "The application of reflected GPS signals to ocean and wetland remote sensing," *Proc. 5th Int. Conf. Remote Sens. Mar. Coastal Environ.*, Vol. 1, 522–529, 1998.

25. Katzberg, S., O. Torres, M. Grant, and D. Masters, "Utilizing calibrated GPS reflected signals to estimate oil reflectivity and dielectric constant: Results from SMEX02," *Remote Sensing of Environment*, Vol. 100, 17–28, 2006.

26. Larson, K. M., J. J. Braun, E. E. Small, V. U. Zavorotny, E. D. Gutmann, and A. L. Bilich, "GPS multipath and its relation to near-surface soil moisture content," *IEEE J-STARS*, Vol. 3, No. 1, 91–99, 2010.

27. Roussel, N., F. Frappart, G. Ramillien, J. Darrozes, F. Baup, L. Lestarquit, and M. C. Ha, "Detection of soil moisture variations using GPS and GLONASS SNR data for elevation angles ranging from 2 to 70," *IEEE J-STARS*, Vol. 9, No. 10, 4781–4794, 2016.

28. Yang, T., W. Wan, X. Chen, T. Chu, and Y. Hong, "Using BDS SNR observations to measure near-surface soil moisture fluctuations: Results from low vegetated surface," *IEEE Transactions on Geoscience and Remote Sensing*, Vol. 14, No. 8, 1308–1312, 2017.

29. Han, M., Y. Zhu, D. Yang, X. Hong, and S. Song, "A semi-empirical SNR model for soil moisture retrieval using GNSS SNR data," *Remote Sensing*, Vol. 10, No. 2, 1–19, 2018.

30. Egido, A., M. Caparrini, G. Ruffini, S. Paloscia, E. Santi, L. Guerriero, N. Pierdicca, and N. Floury, "Global navigation satellite systems reflectometry as a remote sensing tool for agriculture," *Remote*

Sensing, Vol. 4, No. 8, 2356–2372, 2012.

31. Chew, C. C., E. E. Small, K. M. Larson, and V. U. Zavorotny, "Effects of near-surface soil moisture on GPS SNR data: Development of a retrieval algorithm for soil moisture," *IEEE Transactions on Geoscience and Remote Sensing*, Vol. 52, No. 1, 537–543, 2015.

32. Small, E. E., K. M. Larson, and J. J. Braun, "Sensing vegetation growth with reflected GPS signals," *Geophys. Res. Lett.*, Vol. 37, No. 12, 1–5, 2010.

33. Vey, S., A. Güntner, J. Wickert, T. Blume, and M. Ramatschi, "Long-term soil moisture dynamics derived from GNSS interferometric reflectometry: A case study for Sutherland, South Africa," *Gps Solut.*, Vol. 20, No. 4, 641–654, 2016.

34. Wan, W., K. M. Larson, E. E. Small, C. C. Chew, and J. J. Braun, "Using geodetic GPS receivers to measure vegetation water content," *Gps Solut.*, Vol. 9, No. 2, 237–248, 2015.

35. Larson, K. M., E. D. Gutmann, V. U. Zavorotny, J. J. Braun, M. W. Williams, and F. G. Nievinski, "Can we measure snow depth with GPS receivers?," *Geophys. Res. Lett.*, Vol. 36, No. 17, 1–5, 2009.

36. Larson, K. M. and E. E. Small, "Normalized microwave reflection index: A vegetation measurement derived from GPS networks," *IEEE J-STARS*, Vol. 7, No. 5, 1501–1511, 2014.

37. Zavorotny, V. U., K. M. Larson, J. J. Braun, E. E. Small, E. D. Gutmann, and A. L. Bilich, "A physical model for GPS multipath caused by land reflections: Toward bare soil moisture retrievals," *IEEE J-STARS*, Vol. 3, No. 1, 100–110, 2010.

38. Chamoli, V., R. Prakash, A. Vidyarthi, and A. Ray, "Sensitivity of NavIC signal for soil moisture variation," *International Conference on Emerging Trends in Computing and Communication Technologies*, 1–4, IEEE, 2017.

39. Chamoli, V., R. Prakash, A. Vidyarthi, and A. Ray, "Analysis of NavIC multipath signal sensitivity for soil moisture in presence of vegetation," *International Conference on Innovative Computing and Communications*, Vol. 2, 353–364, Springer, Singapore, 2020.

40. Martin, A., S. Ibáñez, C. Baixauli, S. Blanc, and A. Julián, "Multi-constellation GNSS interferometric reflectometry with mass-market sensors as a solution for soil moisture monitoring," *Hydrol. Earth Syst. Sci.*, Vol. 24, 3573–3582, 2020.

41. Yang, T., W. Wan, and X. Chen, "Land surface characterization using BeiDou signal-to-noise ratio observations," *Gps Solut.*, Vol. 23, 32, 2019.